Modeling and Optimization of a Model IV Fluidized Catalytic Cracking Unit

Robert C. Ellis, Xuan Li, and James B. Riggs
Dept. of Chemical Engineering, Texas Tech University, Lubbock, TX 79409

The problem of on-line optimization of a model IV fluidized catalytic cracking (FCC) unit is analyzed. The "process" was modeled by combining a model IV FCC unit dynamic simulator (McFarlane et al., 1993; Khandalekar, 1993) with a ten-lump yield model (Jacob et al., 1976; Arbel et al., 1995) for the reactor section. The steady-state optimization model consisted of macroscopic steady-state models of the regenerator and reactor, a simplified reactor yield model, and models of the various process constraints. The steady-state optimization problem was solved using successive quadratic programming software (NPSOL, Gill et al., 1986) and the optimum process set points were implemented on the process simulator using a nonlinear constraint controller (Kandalekar and Riggs, 1995). The relative performance of constraint control, off-line optimization, and on-line optimization is compared for different feed characteristics and product pricing structures.

Introduction

The FCC unit is a refinery process that converts high-molecular-weight gas oils into more valuable, lighter hydrocarbon products. Since the FCC unit is capable of converting large quantities of heavy feed into more valuable gasoline in a matter of seconds, efficient operation of the FCC unit is essential to the economic health of a refinery. The FCC unit is a multivariable nonlinear process which has a number of operational constraints that limit unit production rates. Since FCC units are economically important and involve complex interactions between product yields and production rates, they are an ideal candidate for optimization.

A number of articles have been written about modeling of an FCC unit. Ford et al. (1976) developed a distributed parameter model of the regenerator in an FCC unit using a detailed kinetic combustion model. Lee and Grove (1985) presented a model of an FCC unit based on macroscopic models of the reactor and regenerator. Monge and Georgakis (1987) developed a dynamic model of an FCC unit and used it to examine the dynamic behavior of the process. McFarlane et al. (1993) developed a dynamic FCC unit model with constraints that was posed as a challenge problem for the chemical process control community. They used a distributed parameter model of the regenerator but used only a continuous stirred-tank reactor (CSTR) for the reactor section, which did not include a yield model. The FCC simulator used in this work is based on a modified version of the McFarlane FCC model. Theologos et al. (1997) used a 3-D fluid flow and reaction yield model of the FCC reactor to investigate the effects of injection geometry on the yield of the desired products.

FCC optimization requires a detailed yield model capable of predicting the yields of valuable products and gasoline octane value. Early FCC yield models predicted feed conversion based on process operating conditions and cracking data for different gas oil feeds (Blanding, 1953). Weekman and Nace (1970) proposed a kinetic-based FCC reaction network consisting of three kinetic lumps, which was later expanded to ten lumps by Jacobs et al. (1976). An updated version of the ten-lump model was proposed by Arbel et al. (1995) that considered modern FCC units and allowed for catalyst characterization based on experimental data. The development of more rigorous, molecular-based, FCC yield models is an area of active research (Liguras and Allen, 1989; Liguras et al., 1992).

The light gases produced by the FCC unit process include hydrocarbons with molecular weights of up to C_5. Light gas correlations based on industrial yield data have been proposed to provide a general description of light gas yields as a

Correspondence concerning this article should be addressed to J. B. Riggs.
Current address of R. C. Ellis: Aspen Technology Inc., 9896 Bissonnet, Houston, TX 97042.

function of feed conversion and feed gravity (Gary and Handwerk, 1983; Maples, 1993). Detailed reaction schemes for the production of light gases have been proposed by John and Wojciechowski (1975) and Corma et al. (1984).

Models used to predict the octane number of gasoline produced in an FCC unit vary in degrees of sophistication. Rigorous molecular-based models have been proposed (Liguras and Allen, 1990), along with correlations developed from industrial data (Maples, 1993). Other sources of octane information from an industrial viewpoint are prevalent throughout the literature (Desai and Haseltine, 1989; Pierce and Logwinuk, 1985; Leuenberger, 1988).

The primary impetus for supervisory optimization of an FCC unit is economic. Successful implementations of unit optimization have been published (Van Wijk and Pope, 1993; Lauks et al., 1993). Dynamic Matrix Control Corporation (DMC) reported that the implementation of an on-line optimization routine to a process will increase unit profitability by 3–5% (DMC, 1990). Other benefits of an on-line optimization routine include smoother constraint handling and off-line "what if" studies.

Process Overview

The FCC process (Figure 1) consists of three subsections: reactor, regenerator, and main fractionator. The reactor of an FCC unit consists of a feed riser line and a catalyst disengaging zone. The riser section is a long vertical pipe which is partially contained in the reactor vessel. After being heated to a temperature of 600–800°F (316–427°C), the gas oil feed is injected into the riser where it is mixed with hot catalyst (1,200–1,400°F, 649–760°C) from the regenerator. The catalyst supplies the reaction sites and thermal energy required to carry out the endothermic catalytic cracking reactions. The temperature of the product and catalyst as it leaves the riser is approximately 900–1,000°F (482–538°C). The residence time for the catalyst in the riser is on the order of 2–10 s. The short residence time minimizes gasoline cracking and catalyst deactivation due to coking, resulting in better yields of the more valuable products. After the catalyst and hydrocarbons exit the riser section the catalyst is removed from the hydrocarbon stream in the disengaging zone of the reactor vessel. The hydrocarbon gas stream is sent to the main fractionator for separation while the spent catalyst returns to the regenerator where a portion of the coke formed during the cracking reactions is removed from the catalyst by combustion with air.

In the regenerator, heated combustion air is mixed with the spent catalyst to burn off the coke produced during the cracking process. Carbon dioxide, carbon monoxide, water, and excess air are released from the regenerator as flue gas. Since the combustion of coke from the catalyst is an exothermic reaction, the regenerated catalyst has increased thermal energy that is required for the cracking reactions in the riser section. The temperatures of the reactor and regenerator will remain stable if the thermal energy balance between the two vessels is satisfied. Energy balance closure will be realized when the thermal energy required to vaporize and crack the gas oil feed is equal to the thermal energy released from the combustion of coke from the catalyst. The excess oxygen in the flue gas is controlled to attain efficient combustion in the regenerator.

The hydrocarbon products from the reactor are separated into various components in the main fractionator. The product streams from the main fractionator include light gases (C_4 and lighter), gasoline, heavy fuel oil (HFO), light fuel oil

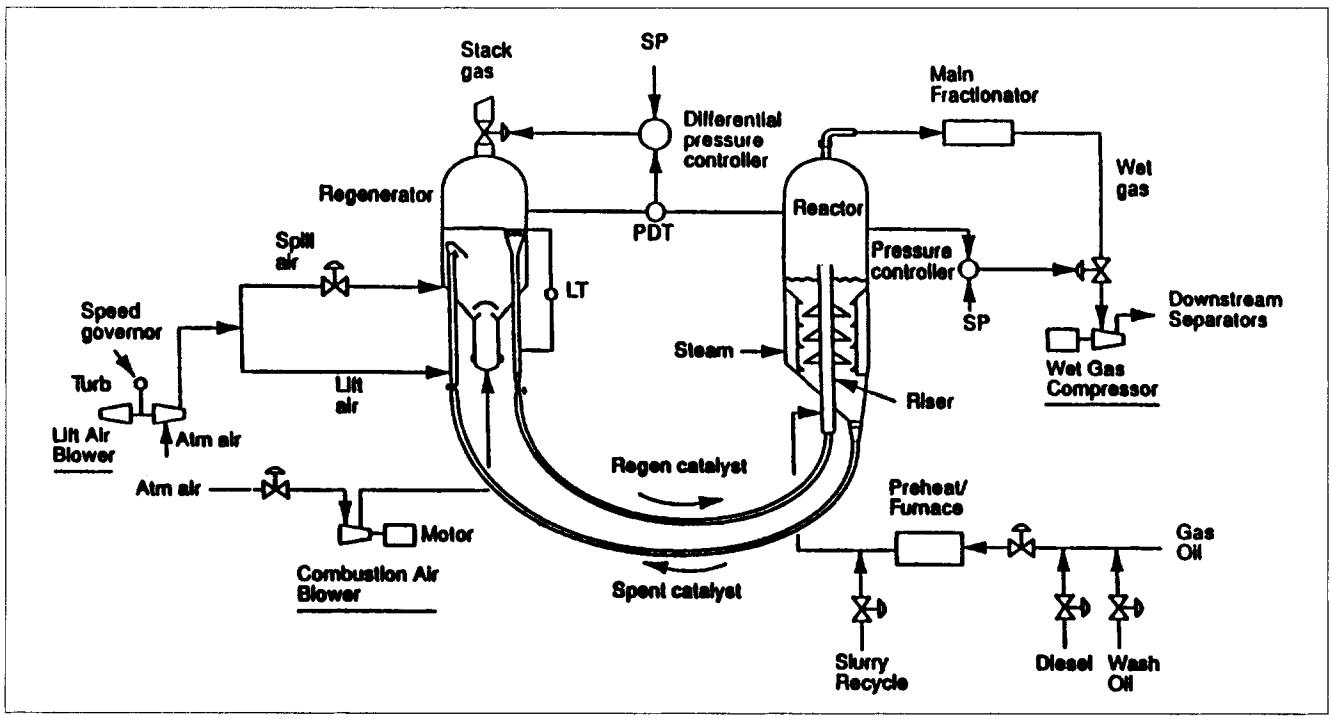

Figure 1. Model IV fluid catalytic cracking unit.

(LFO), cycle oil, and fractionator bottoms. In the current study, HFO and cycle oils are lumped together as a single product.

Overall Approach

The simulation study of on-line optimization of an FCC unit involves a number of different models, both steady-state and dynamic. The "process" is represented by a dynamic model of a model IV FCC unit (McFarlene et al., 1993; Khandalekar, 1993) which is combined with a steady-state yield model for the FCC reactor. The dynamic simulator calculates the time-varying states of the FCC unit at any point in time while the yield model uses the reactor conditions to calculate the conversion and the distribution of products.

The "process"(dynamic simulator and detailed yield model) is controlled by a nonlinear constraint controller. The nonlinear constraint controller uses a steady-state energy balance on the reactor, dynamic energy, and oxygen balances for the regenerator, and models of the various constraints in order to maintain operation at the specified reactor temperature, regenerator temperature, and O_2 level in the flue gas from the regenerator while maximizing the feed rate to the FCC unit.

Finally, the supervisory optimization algorithm (SOA) chooses the set points for the reactor temperature, regenerator temperature, O_2 level in the flue gas from the regenerator, and the process feed rate. The models used in the SOA consist of steady-state FCC unit models, steady-state models of the constraints and an approximate yield model. A successive quadratic programming (SQP) optimization engine uses the SOA models to identify the economic-based optimum operating point.

It should be pointed out that the models used both by the constraint controller and by the SOA are parameterized on-line using "process" data in order to keep the models in agreement with the process when significant process model mismatch occurs.

In summary, the SOA identifies the set points for the constraint controller. Then the constraint controller adjusts the manipulated variables in the "process" in order to maintain operation at the desired operating point. The hierarchy of optimization/constraint control/process model is shown in Figure 2.

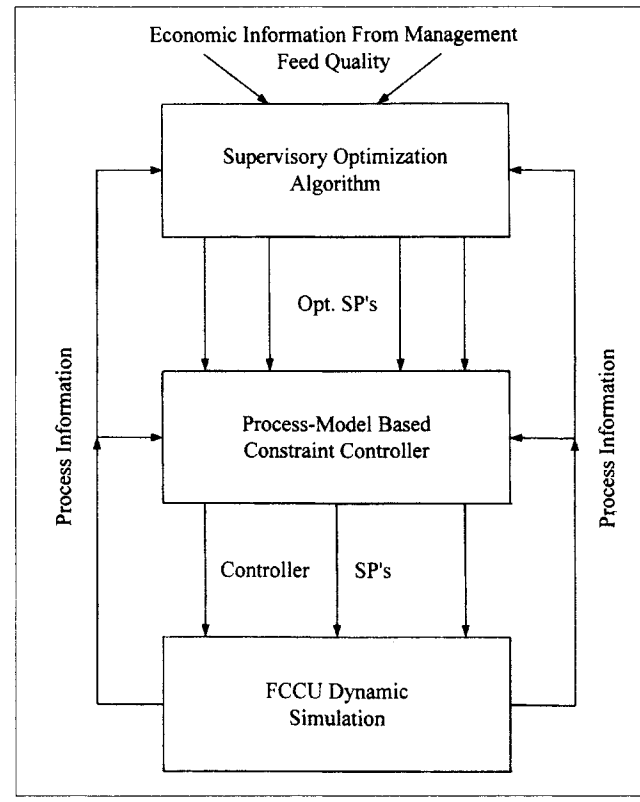

Figure 2. Supervisory optimization flow diagram.

Process Model

The process model consists of the dynamic FCC unit model combined with the detailed yield model for the reactor.

FCC unit dynamic model

The model IV FCC unit dynamic simulator used in this study was originally developed by McFarlane et al. (1993) using ACSL (advanced continuous simulation language). Khandalekar (1993) converted the ACSL code to FORTRAN and benchmarked the simulator against open-loop responses provided in the Amoco/Lehigh University Model IV FCC industrial challenge problem statement (McFarlane et al., 1993).

The mathematical models that make up the FCC unit simulator consist of a set of time-dependent differential equations that were integrated using a fourth-order Runge-Kutta method with a step size of 0.25 s. The regenerator was described using a set of spatial differential equations that were evaluated using an explicit Euler method with a step size of 0.15 ft (0.05 m). To reduce computation time, the differential equations for the regenerator were integrated after every three steps in the time domain without a significant loss of accuracy.

Reactor model

The model by McFarlane et al. (1993) used a continuous stirred-tank reactor (CSTR) model that used empirical parameters to predict conversion, reactor temperature, and coke content of the spent catalyst. In order to study FCC optimization, the CSTR model was replaced by a plug-flow reactor (PFR) model that predicts reactor temperature, the product distribution based on a ten-lump model, the product distribution of the light gases, the coke content on the catalyst, the octane of the gasoline produced assuming pseudo-steady-state operation, and perfect gas oil/catalyst contacting.

The differential material balance equations for the component lumps, the differential energy balance, and the differential material balance for the deposition of coke on the catalyst were integrated along the height of the riser tube using LSODE (Hindmarsh, 1980). LSODE was required to integrate the reactor riser equations due to the stiffness caused by the coke deposition kinetic equations. The temperature of the reaction mixture and the product distribution predicted at the outlet of the riser were used in empirical algebraic equations to calculate the distribution of light gas products and the octane of the gasoline produced.

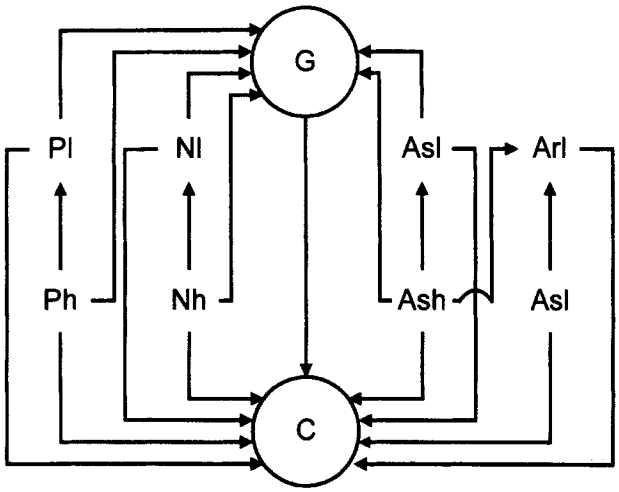

Figure 3. Ten-lump FCC reaction network.

Ten-Lump Model. A ten-lump FCC unit reactor-riser model (Jacob et al., 1976; Arbel et al., 1995) was incorporated into the dynamic simulator to provide a more complete description of the gas oil cracking kinetics. This model characterizes the gas oil feed on the basis of molecular structure and molecular weight. The ten-lump model is shown in Figure 3, and the boiling ranges of the individual lumps are shown in Table 1. The light gas oil (LGO) components with boiling points (1) greater than 648°F (342°C) and (2) between 432°F and 648°F (222°C and 342°C) are each grouped in four lumps: paraffins, naphthenics, aromatics, and aromatics with substituent branches. The heavy gas oil (HGO) has the same four lumps but each lump has a boiling point greater than 648°F (342°C). Gasoline contains C_5s up to a boiling point of 432°F (222°C). The "C" lump contains coke and light gases (C_1 to C_4). The kinetic models used for this reaction network, which were taken from Jacob et al. (1976) and Arbel et al. (1995), assumed first-order reactions with Arrhenius rate constants for each of the 20 reactions shown in Figure 3. The differential material balance for coke deposition on the catalyst in the riser was based on previous work by Voorhies (1945), Gross et al. (1974), and Krambeck (1991). This model used an Arrhenius rate constant and includes a coking tendency factor that was expressed as an empirical function of the local product distribution (Gross et al., 1974).

Table 1. Boiling Range of Lumps in Ten-Lump FCC Reaction Network

Lump	Description	Boiling Range
P_h	wt. % paraffinic molecules	$T > 648$°F*
N_h	wt. % naphthenic molecules	$T > 648$°F*
As_h	wt. % aromatic substituent molecules	$T > 648$°F*
Ar_h	wt. % carbon atoms among aromatic rings	$T > 648$°F*
P_l	wt. % paraffinic molecules	$432 < T < 648$°F**
N_l	wt. % naphthenic molecules	$432 < T < 648$°F**
As_l	wt. % aromatic substituent molecules	$432 < T < 648$°F**
Ar_l	wt. % carbon atoms among aromatic rings	$432 < T < 648$°F**
G	wt. % gasoline	(C5s–432°F)
C	wt. % coke and ...	(C1–C4, and coke)
	1. Butene 4. Propene	
	2. Isobutane 5. Propane	
	3. Butane 6. Gases < C2	

*342°C.
**222–342°C.

Light Gas Model. The light gas model predicts the yields of light gases based on the outlet conditions from the riser and the inlet feed quality while honoring the framework set by the ten-lump model. In order to predict the yields of *n*-butane, butylenes, *i*-butane, propane, propylene, and gases lighter than propane, expressions based on literature data (Gary and Handwerk, 1983) were developed. The feed gravity (API) was estimated based on the composition of the feed, molecular weight information, and carbon-to-hydrogen ratio using standard correlations (Winn, 1957). These gas yields were scaled for consistency with the ten-lump yield model by selecting the value of K. The expressions for the light gases were estimated using the following equations:

for butane

$$\text{wt.}_{n-\text{butane}} = K\frac{\rho_{n-\text{butane}}}{\rho_{\text{feed}}}(0.037424X_v - 0.06856\ \text{API} + 0.909615), \quad (1)$$

for butylenes

$$\text{wt.}_{\text{butylene}} = K\frac{\rho_{\text{butylene}}}{\rho_{\text{feed}}}(0.1476X_v - 0.06067\ \text{API} - 1.69867), \quad (2)$$

for *i*-butane

$$\text{wt.}_{i-\text{butane}} = K\frac{\rho_{i-\text{butane}}}{\rho_{\text{feed}}}(0.101X_v - 0.098667\ \text{API} - 4.20733), \quad (3)$$

for propylene

$$\text{wt.}_{\text{propylene}} = K\frac{\rho_{\text{propylene}}}{\rho_{\text{feed}}}[(1.366\ \text{EXP}(0.01956X_v) + 0.26125\ \text{API} - 6.00875)], \quad (4)$$

for propane

$$\text{wt.}_{\text{propane}} = K\frac{\rho_{\text{propane}}}{\rho_{\text{feed}}}[0.36089\ \text{EXP}(0.02655X_v)], \quad (5)$$

for C_2 gases and lighter gases

$$\text{wt.}_{c_2s} = K\frac{\rho_{c_2s}}{\rho_{\text{feed}}}[0.366\,\text{EXP}(0.03322X_v) - 0.310\ \text{API} + 7.13]. \quad (6)$$

Gasoline Octane Model. The motor octane number (MON) was estimated using information from the literature (Leuenberger, 1988; Desai and Haseltine, 1989) and the expression is shown below.

$$\text{MON} = 72.5 + 0.05(T_r - 900°\text{F}) + 0.17(X_{\text{wt.}} - 0.55) \quad (7)$$

The research octane number (RON) was determined using a correlation developed from literature data (Gary and Handwerk, 1983).

$$\text{RON} = 1.2931\,\text{MON} + 12.06897 \quad (8)$$

Modeling benchmarking

The process model was quantitatively benchmarked (Kandalekar and Riggs, 1995) against the results presented by McFarlane et al. (1993). In addition, the yield model and octane model were qualitatively benchmarked against published data. A comparison between the predications from the yield model developed in this work and published results versus conversion were made for C_4 yields (Nelson, 1973; Voorhies et al., 1964; Wachtel et al., 1972; Maples, 1993), C_3 yields (Maples, 1993), gasoline yield (Khandalekar, 1993), coke yields (Maples, 1993), and motor octane number (Desai and Haseltine, 1989). These results show a good representation of the available data by the yield and octane models. For the specific comparisons between the model and the published data, see Ellis (1996).

Nonlinear Constraint Controller

The nonlinear multivariable constraint controller used in this study is based on using generic model control (Lee and Sullivan, 1988). This constraint controller is designed to maximize unit feed rate for a particular operating point by maintaining operation against the operative constraints while maintaining the reactor temperature, regenerator temperature, and the oxygen constant for the flue gas at their respective set points. For a detailed description of the constraint controller, the reader is referred to Khandalekar and Riggs (1995).

Process models

The constraint controller uses a macroscopic steady-state energy balance for the reactor, and macroscopic dynamic energy and oxygen balances on the regenerator. The adjustable model parameters (enthalpy of gas oil cracking, ΔH_{crack}, and the frequency factor for coke combustion) were updated with on-line data using the nonlinear model parameterization approach used by Rhinehart and Riggs (1991).

Constraint models

The constraint controller considers the following constraints which were set by McFarlane et al. (1993):

(1) Maximum tube temperature in the firebox.
(2) Maximum fuel flow rate to the firebox.
(3) Maximum catalyst circulation rate (ΔP).
(4) Maximum regenerator air flow rate.
(5) Maximum flow rate through the wet gas compressor.

Nonlinear models were used to model each of these constraints. The operative constraint was used to set the gas oil feed rate to the process. It should be pointed out that the maximum flow rate through the wet gas compressor used in the study was 10% lower than the value specified by McFarlane et al. (1993). This was done in order that the wet gas compressor would act as an operative constraint.

Supervisory Optimization Algorithm

The supervisory optimization algorithm (SOA) is the highest level in the process/controller/optimization hierarchy and determines the economic optimum operating point for the FCC unit. The SQP algorithm, used to solve the optimization problem, consists of the economic objective function, the collection of process constraints, and the optimization engine uses four decision variables.

The regenerator temperature, riser temperature, gas oil feed flow rate, and stack gas oxygen concentration were chosen as decision variables for optimization. The four equations used to describe the FCC unit were solved simultaneously for four process variables using Newton's method (Riggs, 1994). The remaining process variables were determined using explicit expressions and then the objective function value was evaluated. The economic objective function used in this study is shown below

$$F = \left[\sum_{i=1, i \neq 9-12}^{18} p_i \text{wt.}_i + (p_9 + p_{\text{oct}} f_{\text{oct}})\text{wt.}_9 - p_{\text{feed}} \right] F_{\text{oil}} \quad (9)$$

$$f_{\text{oct}} = \frac{\text{MON} + \text{RON}}{2} - 85.69 \quad (10)$$

The values for p_i are based on the economic climate and are tabulated in Table 2 for the various cases evaluated in this study. The economic optimization problem was also subject to the process constraints. In addition to the constraints previously listed, there were upper and lower limits placed on both independent and dependent variables in the FCC unit process. Table 3 lists the upper and lower limits for the constrained variables considered here.

Optimization model for the FCC unit

The FCC unit model used for process optimization was de-

Table 2. Product Prices for Three Modes of Operation Studied*

Mode	p_{HFO}	p_{LFO}	p_{gasoline}	p_{nC_4}	$p_{=\text{C}_4}$	p_{iC_4}	$p_{=\text{C}_3}$	p_{nC_3}	$p_{\leq \text{C}_2}$	p_{octane}
Gasoline	0.02773	0.07203	0.09716	0.05695	0.08496	0.07903	0.09547	0.05579	0.0600	0.00348
LFO	0.02828	0.10084	0.09230	0.05695	0.08496	0.07903	0.09547	0.05579	0.0600	0.00116
Lt. Gas	0.02773	0.07203	0.08097	0.07909	0.09346	0.08448	0.09984	0.05582	0.0660	0.00116

*Note: Values are expressed as \$/lb except for p_{octane}, which is \$/octane.

Table 3. Process Constraint Used in Optimization

Constraint Number	Lower Bound	Process Variable	Upper Bound
1	1,265°F	T_{reg}	1,400°F
2	980°F	T_r	994°F
3	75 lb/s	F_{oil}	132 lb/s
4	0.500%	$O_{2,sg}$	2%
5	650°F	T_3	1,700°F
6	0	F_5	39.5 SCM
7	14.7 psig	P_4	54 psig
8	14.7 psig	P_6	54 psig
9	5,100 RPM	*sa*	6,100 RPM
10	0	$F_{sucn,lift} - F_{surge,lift}$	None
11	−5 psia	$P_6 - P_4$	2 psia
12	0	L_{sp}	20 ft
13	45,000 SCFM	$F_{sucn,comb}$	55,000 SCFM
14	0	F_{wg}	0.90 lb mol/s

SI conversion: °C = (°F − 32)/1.8; kg = lb = 0.454; kPa = psi × 6.89; L/s = CFM × 0472.

veloped using macroscopic steady-state phenomenological models and empirical expressions. The models and expressions that comprise the optimization model are presented in the following order:

(1) Reactor-riser
(2) Reactor yield model
(3) Regenerator
(4) Firebox and preheat furnace
(5) Pressure balances

Reactor-Riser. A reactor-riser macroscopic, steady-state energy balance was used to develop an approximate model for the reactor-riser. The reactor model assumes that the heat lost by the regenerated catalyst and the feed is equal to the heat consumed by the cracking reaction occurring in the riser

$$F_{rgc}C_{p,c}(T_{reg} - T_r) + F_{oil}C_{p,oil}(T_2 - T_r) - F_{oil}X_{wt.}\Delta H_{crack} = 0 \tag{11}$$

The gas oil conversion $X_{wt.}$ is estimated using the following expression developed by Khandalekar and Riggs (1995)

$$X_{wt.} = 1 - \frac{k_2 t_c}{k_2 t_c - k_1 t_c \,\mathrm{COR}(e^{-k_2 t_c} - 1)e^{-E_F/T}_{r,avg}} \tag{12}$$

$$T_o = \frac{F_{rgc}C_{p,c}T_{reg} + F_{oil}C_{p,oil}T_2}{F_{rgc}C_{p,c} + F_{oil}C_{p,oil}} \tag{13}$$

$$T_{r,avg} = 0.3T_o + 0.7T_r \tag{14}$$

Reactor-Yield Model. A simplified version of the ten-lump yield model, which was used for the "process," was used by the SOA. The simplified model used two assumptions which were designed to make the simplified yield model more tractable.

(1) The average riser temperature $T_{r,avg}$ was used to evaluate rate constants.

(2) The coke on the catalyst in the reactor was assumed to remain constant. A weighted average was used between the top and bottom of the riser.

These assumptions allowed for the direct calculation of the reactor yield from the operating conditions in the reactor-riser and provided for some structured mismatch between the detailed yield model and the simplified yield model which was used by the SOA.

Regenerator. Steady-state macroscopic energy and oxygen balances were used to develop expressions to determine the regenerator temperature and excess oxygen in the flue gas. Several assumptions were made in the development of the regenerator model.

(1) The combustion of coke was modeled using the following reaction:

$$C + O_2 \rightarrow CO_2.$$

(2) The depletion of oxygen across the regenerator bed was modeled as a plug-flow reactor. (Note that the constraint controller modeled the regenerator as a CSTR.)

(3) With regard to coke content on the catalyst, the catalyst bed was assumed to be a well-mixed CSTR; therefore, the concentration of carbon on the catalyst was assumed constant throughout the catalyst bed.

(4) No reaction occurs in the dilute phase of the regenerator, above the catalyst bed.

These assumptions made it possible to obtain a tractable regenerator model at the expense of process/model mismatch.

The steady-state energy balance for the regenerator is shown below

$$F_{rgc}C_{p,c}(T_r - T_{reg}) + F_{air}C_{p,air}(T_{air} - T_{reg})\frac{F_{air}O_{2,air}}{29} + \left[1 - \exp\left(\frac{-100k\rho_B C_{rgc} z_{bed}}{v_s}\right)\right]\Delta H_{coke} = 0.0 \tag{15}$$

$$k = k_{O_2}\exp\left[\frac{-34138.4}{T_{reg} + 460}\right]$$

An empirical expression for the concentration of carbon on regenerated catalyst as a function of flue gas oxygen concentration and regenerator temperature was developed by Cutler (1990)

$$C_{rgc} = C_{rgc,ref}\left[\frac{LM(O_{2,air}, O_{2,ref})}{LM(O_{2,air}, O_{2,sg})}\right]\exp\left[\frac{E}{R}\left(\frac{1}{T_{reg}} - \frac{1}{T_{reg,ref}}\right)\right] \tag{16}$$

where

$$LM(x,y) = \frac{(x-y)}{\ln\left(\frac{x}{y}\right)}$$

Steady-state reference parameters were determined using state simulation data and nonlinear regression. The approximate model for estimation of the concentration of carbon on spent catalyst was offered by Lee et al. (1985).

$$C_{sc} = C_{rgc} + \sqrt{\frac{k_c \exp(-E_{cf}/RT_r)}{C_{rgc}^{0.4}}} \tag{17}$$

The steady-state oxygen balance for the regenerator is determined by equating the reduction in the moles of oxygen in the air fed to the regenerator with the number of moles of oxygen consumed by the coke combustion reaction

$$C_3 F_{rgc}(C_{sc} - C_{rgc}) = F_{air}(0.21 - O_{2,sg}) \tag{18}$$

where C_3 is 2.78 based on assuming the complete combustion of coke and the coke composition as CH.

Preheat Furnace. The preheat furnace is used to heat the gas oil feed prior to entering the reactor-riser reaction. The macroscopic energy balance around the preheat furnace is given by

$$Q_{total} = Q_{trans} + Q_{loss} \tag{19}$$

where Q_{total} is determined based on assuming complete combustion of the fuel; Q_{trans} is calculated using a log mean temperature difference; and Q_{loss} is modeled as directly proportional to the heat load in the firebox. Therefore, this equation becomes

$$F_5 \Delta H_u = UA_f LM(T_3, T_1) + aF_5 T_3 \tag{20}$$

In addition, the heat absorbed by the feed, Q_{trans}, is also equal to the sensible heat change of the feed.

$$UA_f LM(T_3, T_1) = F_{oil} C_{p,oil}(T_2 - T_1) \tag{21}$$

Equation 21 is used to calculate the firebox temperature, T_3. Then Eq. 20 is used to calculate the fuel flow rate to the firebox. If the upper limit on T_3 is exceeded, T_3 is set to its upper limit. If F_5 is in excess of its upper limit, F_5 is set at its upper limit and F_{oil} is calculated from the simultaneous solution of Eqs. 20 and 21.

Pressure Distribution/Flow Calculations. The air injection to the regenerator and the stack gas valve maintain the pressure in the regenerator. The pressure difference between the reactor and the regenerator and the height of catalyst in the stand pipe are used to transport catalyst to the reactor. The gaseous products are produced in the reactor flow to the main fractionator driven by pressure difference. The LFO and HFO are separated in the main fractionator. Gasoline and light gases are separated in the main fractionator and leave from the overhead of the main fractionator to the suction side of the wet gas compressor. The pressure distribution through an FCC unit is maintained by the valves on the regenerator air blowers, regenerator stack gas valve, wet gas compressor suction valve, and bypass valve. In the simulator, the reactor pressure was maintained constant by adjusting the wet gas compressor suction valve. A constant pressure drop between the main fractionator and the reactor is assumed. The regenerator pressure and wet gas compressor suction pressure are updated based on assumed fluid dynamics.

The total air-flow rate to the regenerator F_{air} is specified as a degree of freedom by the constraint controller. Since the sum of the lift air F_{la} and combustion air F_{ca} must equal the total air-flow rate, F_{la} and F_{ca} are set as follows (McFarlane et al., 1993)

for $F_{air} < 58.94$ lb/s (17.96 kg/s)

$$F_{la} = 12.41 \text{ lb/s } (3.78 \text{ kg/s})$$

$$F_{ca} = 46.53 \text{ lb/s } (14.18 \text{ kg/s})$$

for 58.94 lb/s (17.96 kg/s) $< F_{air} <$ 66.07 lb/s (20.14 kg/s)

$$F_{ca} = 46.53 \text{ lb/s } (14.18 \text{ kg/s})$$

$$F_{la} = F_{air} - F_{ca}$$

for $F_{air} \geq 66.07$ lb/s (20.14 kg/s)

$$F_{la} = 19.54 \text{ lb/s } (5.96 \text{ kg/s})$$

$$F_{ca} = F_{air} - F_{la} \tag{22}$$

Since the regenerator pressure remains relatively constant during normal operation, its measured value was assumed constant for optimization calculations. The pressure drop/flow equations for the air blowers were used along with the effect of catalyst weight (McFarlane et al., 1993) to calculate the pressure at the bottom of the catalyst bed.

For the wet gas compressor, the ratio of the wet gas flow rate to the reactor feed rate is empirically modeled as a function of the reactor temperature

$$F_{wg}/F_{oil} = C_1 + C_2(T_r - T_{r,ref}) \tag{23}$$

The flow/pressure drop equations for the wet gas compressor presented by McFarlane et al. (1993) are then used to calculate the inlet pressure to the wet gas compressor. The pressure drop between the wet gas compressor and the main fractionator was calculated using the flow equation given by McFarlane et al. (1993). Finally, the reactor pressure was calculated by assuming a constant pressure drop between the reactor and the main fractionator (McFarlane et al., 1993).

Solution Procedure for Optimization Model. The optimization engine selects the four degrees of freedom (T_{reg}, T_r, F_{oil}, and $O_{2,sg}$) and with these values the model equations are solved simultaneously for all the needed steady-state operating conditions for the FCC unit. The reactor conditions are then used to calculate the distribution of products produced by the reactor using the approximate yield model. Finally, the product prices and octane value are combined with the product flow rates to calculate the economic objective function values. Also, the process operating conditions are used to calculate the values of the process constraints.

In order to solve for the steady-state operating conditions, Newton's method (Riggs, 1994) is used to solve a black-box function of four unknowns: T_2, T_3, F_{rgc}, F_{air}.

This black-box function is implemented in the following sequence:

(1) Determine combustion and lift air flow rates (Eq. 22).

(2) Calculate the pressure distribution through the FCC unit.

(3) Using Eqs. 12, 13, and 14, calculate the gas oil conversion, $X_{wt.}$

(4) Calculate the amount of coke on the regenerated catalyst, C_{rgc}, using Eq. 16.

(5) Calculate the amount of coke on the spent catalyst using Eq. 17.

(6) Determine the error in the furnace heat balance equation (Eq. 21).

(7) Determine the error in the steady-state energy balance for the regenerator Eq. 15.

(8) Determine the error in the steady-state oxygen balance on the regenerator Eq. 18.

(9) Determine the error in the steady-state energy balance on the reactor Eq. 11.

Summarizing, Newton's method selects values of T_2, T_3, F_{rgc}, and F_{air} until Eqs. 21, 15, 18, and 11 are simultaneously satisfied.

After the four-dimensional black-box function is solved, the approximate reactor yield model is evaluated to calculate the distribution of products. The economic objective function can then be calculated directly. Also, with the process conditions calculated from the solution of the black-box function, each of the process constraints can be evaluated.

Model parameterization

Benefits of FCC unit optimization can only be realized if the FCC unit optimization model accurately describes the FCC process. To reduce process-model mismatch, adjustment parameters, which were common to the process and optimization model and whose exact values were not precisely known, were identified and updated.

Certain parameters were set based on on-line updating and certain parameters were evaluated off-line. The parameters k_{O_2} [preexponential for coking kinetics (Eq. 15)] and k_2 [rate constant for the three-lump model (Eq. 12)] were evaluated off-line. These parameters were estimated using steady-state data from the process simulator using a least squares analysis.

The following parameters were updated on-line:

- k_c—frequency factor for coke formation (Eq. 17). The value of k_c is calculated each time the constraint controller is called ($T = 0.5$ minutes). The value of k_c is filtered using a first-order exponential filter with filter value of 0.05.
- ΔH_{crack}—heat of cracking (Eq. 11). The value of ΔH_{crack} is calculated using the reactor energy balance (Eq. 1) each time the constraint controller is called ($T = 0.5$ minutes). The value of ΔH_{crack} is filtered using a first-order exponential filter with a filter value of 0.05.
- k_1—frequency factor for gasoline formation (Eq. 12). The conversion is estimated on-line by using the product flow rates from the main fractionator ($X_{wt.} = F_{gasoline}/F_{product}$). Eq. 12 can then be used to calculate k_1. This value of k_1 is calculated once every 10 minutes and filtered with a first-order exponential filter with a filter factor of 0.01.

It should be pointed out that both ΔH_{crack} and k_1 are being adjusted using the reactor energy balance. Since ΔH_{crack} is being updated on a much higher frequency than k_1, ΔH_{crack} is really responsible for removing mismatch for the reactor energy balance, while k_1 is slowing tracking conversion changes.

Process-model mismatch between the simulation product yields and the optimization yield model was minimized by adjusting the frequency factors in the optimization yield model. In order to reduce the dimensionality of the parameterization problem, the FCC unit products were grouped as HFO, LFO gasoline, and light gases. Six parameters were used to adjust the frequency factors such that the yields predicted by the optimization yield model were consistent with the process data. The frequency factors were multiplied by the adjustable parameters. Filtered process yield data were used as parameterization targets. The SQP optimization algorithm NPSOL (Gill et al., 1986) was used to determine the adjustable frequency factors based on minimizing the sum of the squares of the errors between the predicated product yields and the measured product flows from the main fractionator.

The product of the yield model frequency factors and the six parameters was used to adjust the ten-lump optimization yield model frequency factors. This parameterization was implemented prior to each optimization cycle.

Results

Table 4 lists a comparison between the gains obtained from the process simulator and the optimization model at the base case conditions for feed API equal to 27. Each of the gains for the three outputs (reactor temperature, regenerator temperature, and oxygen in the flue gas) and the three inputs (fuel flow rate to feed preheater, flow rate of regenerated catalyst, and air flow to the regenerator) show reasonable agreement between the simulator and the optimization model. The diagonal gains (i.e., $\Delta T_r/\Delta F_5$, $\Delta T_{reg}/\Delta F_{rgc}$, and $\Delta O_{2,sg}/\Delta F_{air}$) have better agreement than the off-diagonal gains. These results indicate that the optimization model is reasonable, but there is significant difference between the process simulator and the approximation model that is used to optimize the process simulator.

Table 5 shows the effect of parameter variation on the change in the optimal objective function. The results were obtained by optimizing the process simulator using the optimization model with different optimization model parameters. Note that the optimization objective function is most sensitive to changes in k_{O_2} and reasonable variations in other model parameters have a relatively small effect on the optimum objective function value.

Table 4. Comparison Between the Gains Obtained from the Simulator and Optimization Model at Base Case Conditions, API = 27

	$\Delta PV/\Delta F_5$	$\Delta PV/\Delta F_{rgc}$	$\Delta PV/\Delta F_{air}$
ΔT_r, simulator	−0.552°F/(ft³/s)	0.057°F/(lb/s)	0.070°F/(lb/s)
ΔT_r, model	−0.334°F/(ft³/s)	0.041°F/(lb/s)	0.449°F/(lb/s)
ΔT_{reg}, simulator	1.460°F/(ft³/s)	−0.122°F/(lb/s)	−1.838°F/(lb/s)
ΔT_{reg}, model	0.599°F/(ft³/s)	−0.173°F/(lb/s)	−1.598°F/(lb/s)
$\Delta O_{2,sg}$, simulator	−0.096 mol %/(ft³/s)	0.013 mol %/(lb/s)	0.089 mol %/(lb/s)
$\Delta O_{2,sg}$, model	−0.236 mol %/(ft³/s)	0.036 mol %/(lb/s)	0.101 mol %/(lb/s)

SI conversion: °C = (°F − 32)/1.8; L/s = ft³/s × 28.3.

Table 5. Summary of Results from Sensitivity Analysis Study: The Effect of Parameter Uncertainty on Optimal Objective Value

Change in Parameter	T_{reg}, °F	T_r, °F	F_{oil}, lb/s	$\%O_{2,sg}$	ΔObj. F, %
$k_1 + 7.5\%$	1,265	994.00	104.12	0.5	0.067
$k_1 - 7.5\%$	1,265	993.70	104.27	0.5	−0.111
$k_c + 5.0\%$	1,265	991.63	104.18	0.5	−0.111
$k_c - 5.0\%$	1,265	994.00	104.12	0.5	−0.223
$\Delta H_{crack} + 2.5\%$	1,265	994.00	104.12	0.5	0.089
$\Delta H_{crack} - 2.5\%$	1,265	994.00	104.12	0.5	−0.089
$k_{O_2} + 5.0\%$	1,265	991.60	105.32	0.5	0.200
$k_{O_2} - 5.0\%$	1,265	994.00	104.12	0.5	−0.601

SI conversion: °C = (°F − 32)/1.8; kg = lb × 0.454.

Table 6 shows the sensitivity of the economic objective function to specified changes in the reactor temperature, regenerator temperature, oxygen in the flue gas, and feed flow rate to the FCC unit. Note that the change in the oxygen level in the flue gas has the least effect on the unit profitability while the riser temperature has the largest effect on the profitability.

Table 6. FCC Unit Objective Function Sensitivity Gain Analysis, Feed API = 27, Gasoline Mode

Run	T_r, °F	T_{reg}, °F	$\%O_{2,sg}$	F_{oil}, lb/s	ΔObj. F, %
Base	992	1,270	0.750	102	
ΔT_r	994	1,270	0.750	102	1.105
ΔT_{reg}	992	1,268	0.750	102	0.276
$\Delta O_{2,sg}$	992	1,270	0.850	102	0.069
ΔF_{oil}	992	1,270	0.750	104	0.437

SI conversion: °C = (°F − 32)/1.8; kg = lb × 0.454.

Table 7 compares the optimization performance for base case operation, constraint control, off-line optimization, and the "true" optimum. The base case operation assumed operation at fixed levels in the decision variables (T_{reg} = 1,270°F, T_r = 994°F, $\%O_{2,sg}$ = 0.75) and a fixed feed rate (for API = 27, F_{oil} = 102 lb/s; for API = 23, F_{oil} = 105 lb/s). Constraint control maintains the same values for the decision variable at the base case but maximizes F_{oil} while observing all constraints. Off-line optimization results were obtained by using the constraint controller to maximize the oil feed rate while using the optimization model to determine the optimum values for the decision variables. The off-line optimization results were

Table 7. Comparison of Base Case, Constraint Control, Off-line Optimization, and True Optimum

Case Number	API	Mode	Approach	T_{reg} (°F)	T_r (°F)	F_{oil} (lb/s)	$\%O_{2,sg}$	ΔObj. F	Active Constraints
1	27	Gasoline	Base	1,270	994	102	0.75		
			Constraint control	1,270	994	104.12	0.75	1.13%	5, 14
			Off-line optimization	1,265	994	104.12	0.5	1.82%	5, 14
			Opt. using simulator	1,265	994	104.12	0.5	1.82%	5, 14
2	23	Gasoline	Base	1,270	990	105	0.75		
			Constraint control	1,270	990	109.4	0.75	0.77%	5, 14
			Off-line optimization	1,265	994	107.36	0.786	5.62%	5, 14
			Opt. using simulator	1,265	994	107.36	0.786	5.62%	5, 14
3	23C	Gasoline	Base	1,270	990	105	0.75		
			Constraint control	1,270	990	109.38	0.75	0.77%	5, 14
			Off-line optimization	1,267.12	994	107.36	0.5	4.95%	5, 13, 14
			Opt. using simulator	1,267	994	107.37	0.5	4.97%	5, 13, 14
4	27	LFO	Base	1,270	994	102	0.75		
			Constraint control	1,270	994	104.12	0.75	1.46%	5, 14
			Off-line optimization	1,265	991.9	105.11	0.745	2.04%	5, 14
			Opt. using simulator	1,265	992	105.09	0.75	2.01%	5, 14
5	23	LFO	Base	1,270	990	105	0.75		
			Constraint control	1,270	990	109.4	0.75	1.98%	5, 14
			Off-line optimization	1,265	992.8	107.7	0.885	3.75%	5, 14
			Opt. using simulator	1,265	992.6	107.9	0.874	3.68%	5, 14
6	23C	LFO	Base	1,270	990	105	0.75		
			Constraint control	1,270	990	109.38	0.75	1.22%	5, 14
			Off-line optimization	1,267.12	994	107.36	0.5	4.38%	5, 13, 14
			Opt. using simulator	1,267	994	107.37	0.5	4.35%	5, 13, 14
7	27	Lt. Gas	Base	1,270	994	102	0.75		
			Constraint control	1,270	994	104.12	0.75	1.39%	5, 14
			Off-line optimization	1,265	994	104.12	0.5	1.94%	5, 14
			Opt. using simulator	1,265	994	104.12	0.5	1.94%	5, 14
8	23	Lt. Gas	Base	1,270	990	105	0.75		
			Constraint control	1,270	990	109.4	0.75	1.57%	5, 14
			Off-line optimization	1,265	994	107.36	0.786	4.09%	5, 14
			Opt. using simulator	1,265	994	107.36	0.5	4.09%	5, 14
9	23C	Lt. Gas	Base	1,270	990	105	0.75		
			Constraint control	1,270	990	109.38	0.75	1.57%	5, 14
			Off-line optimization	1,267.12	994	107.36	0.5	4.09%	5, 13, 14
			Opt. using simulator	1,267	994	107.37	0.5	4.23%	5, 13, 14

obtained by parameterizing the optimization models for each case study and using the resulting models to determine the optimum operating conditions. The true optimization results were obtained by allowing the SQP optimizer to select the degrees of freedom and then applying these degrees to the process simulator until the simulation lined out at steady-state. The steady-state results were used to calculate the value of the economic objective function and the constraint values. The SQP optimizer used the objective function value and constraint values to select new values for the degrees of freedom until an optimum set of operating conditions was determined.

Nine separate cases are considered. Three different sets of economic parameters are considered (gasoline, LFO, and light gas modes, see Table 2). For each mode, three different feed types were considered: API = 27; API = 23; and API = 23 with coking tendency increased by 5%.

The changes in objective function value (Δ Obj. F) from base case conditions were based on results obtained from the process simulator. Note that in all cases, the results for off-line optimization were essentially equivalent to the true optimum results. For the gasoline mode, the results for constraint control showed an average increase in profitability over base case operation of 1%, while for the LFO and light gas modes, the increase in profitability was about 1.5%. The average incremental benefit for off-line optimization over constraint control for feed with API = 27 was 0.6%. The average incremental benefit for off-line optimization over constraint control for both cases with API = 23 was over 3%.

In all cases, the wet gas compressor constraint and the preheater tube temperature constraint were operative. For the three cases in which the coking factor was increased, the air blower constraint was also encountered. When the wet gas compressor and the air blower constraints are both operative, the optimizer will drive the process to a system pressure such that there is a proper compromise between these constraints. As system pressure is increased, the wet gas compressor capacity will increase but the combustion air blower capacity will decrease.

All cases except cases 4 and 5 resulted in a reactor temperature at the maximum level (994°F, [532°C]). Since the wet gas compressor constraint is operative at the maximum riser temperature, decreasing the riser temperature results in an increase of the FCC unit feed rates. In the LGO mode (i.e., winter pricing structure), lower riser temperatures result in large feed rate increases and more profitable operation. Some variation in the optimum O_2 in the flue gas was observed although this decision variable does not have a major effect on process profitability. In addition, small changes in the optimum T_{reg} were observed for the case in which the coking tendency of the feed increased.

Figure 4 shows a comparison between off-line and on-line optimization. The off-line results were based on applying constraint control with the optimization decision variables set at optimum levels (see Table 7) for LGO mode for an API of the feed equal to 23. On-line optimization uses model parameterization in order to respond to changes in the process. Initially, both cases are operated at base case conditions. At time equal to 267 minutes, both on-line and off-line optimization are applied with constraint control. After some startup variations, both optimizers line out with a 3.3% improvement over base case operation. At time equal to 420 minutes, the coking tendency of the feed is increased by 3%. Note that after 50 minutes the on-line approach results in about 0.8% more profitable operation than the off-line approach. At time equal to 545 minutes, the coking tendency is returned to its original value and the off-line and on-line results become equal again.

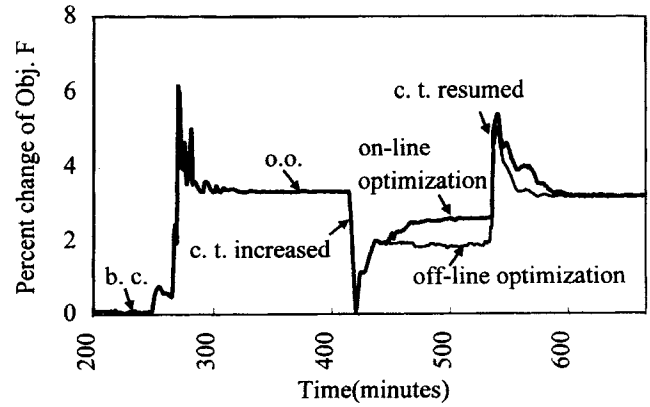

Figure 4. Comparison of on-line optimization with off-line optimization.

b.c.—base case; c.t.—coking tendency; o.o.—optimum operation.

Additional Discussion on FCC Optimization

The model IV FCC unit that was considered in this paper has a number of very specific characteristics, especially with regard to the process constraints. Each FCC unit has its own particular set of constraints. Since the optimum of an FCC unit involves operation on the constraints, the specific combination of constraints will determine which constraints are operative during optimal operation. For example, the maximum firing rate for the feed furnace can severely restrict the FCC processing rate when the wet gas compressor is overdesigned or can be a nonfactor when the wet gas compressor is underdesigned.

A model IV FCC unit is an older design that does not have a slide valve for controlling the catalyst circulation rate and is not constructed of materials that allow higher riser temperatures. The slide valve provides an extra degree of freedom. In effect, the slide valve allows operation against the air blower constraint more frequently than for a Model IV FCC unit. In addition, the slide valve protects against flow reversal in the transfer lines and thus allows for operation closer to the flow reversal limit. The higher riser temperatures provide higher reactor conversion. In certain cases, the maximum reactor temperature may be such that over-cracking of the gasoline may result, significantly reducing gasoline yield. In such cases, it is usually more profitable to operate at reactor temperatures that are less than the maximum even for the gasoline mode. In such cases, the incremental benefit of on-line optimization would be expected to be larger than observed in this study based on the results that were developed for the winter mode for this study.

In this work, several constraints that are commonly encountered in industrial FCC operation were not considered. For example, this work did not model the main fractionator.

Main fractionator flooding can be an operative constraint for an FCC optimization. Also, constraints of FCC operation can result due to constraints in the gas recovery unit, that is, the series of columns responsible for separating the light gas produced by the FCC unit. In addition, the effect of ambient temperature changes on the capacity of the wet gas compressor was not modeled, but can be important for industrial FCC units.

Conclusion

This study has examined a wide range of operation of a model IV FCC unit. It was shown that constraint control and off-line optimization each provide significant incremental economic benefit. On-line optimization is shown to provide an additional improvement when unmeasured changes in the coking tendency of the feed occur.

Notation

a = furnace heat loss parameter, 1.535×10^{-4} Btu/SCF/°F
$C_{p,\text{air}}$ = heat capacity of air, 0.244 Btu/lb/°F
$C_{p,c}$ = heat capacity of catalyst, 0.31 Btu/lb catalyst/°F
$C_{p,\text{oil}}$ = heat capacity of gas oil feed, 0.74 Btu/lb catalyst/°F
C_{rgc} = weight fraction of coke on regenerated catalyst, lb coke/lb catalyst
$C_{\text{rgc,ref}}$ = weight fraction of coke on regenerated catalyst reference, lb coke/lb catalyst
C_{sc} = weight fraction of coke on spent catalyst, lb coke/lb catalyst
C_1 = wet gas production parameter, 0.0088438 lb mol/lb feed
C_2 = wet gas production parameter, 0.00004 lb mol/lb feed/°F
C_3 = constant in the oxygen balance expression, 2.78
E = activation energy of coke combustion reaction, Btu/lb mol
E_{cf} = activation energy of coke formation reaction, Btu/lb mol
E_F = activation energy for conversion of feed in three-lump model, Btu/lb mol
f_{oct} = octane differential used in objective function evaluation, octane number
F = economic objective function for optimization, $/s
F_{air} = air flow rate into regenerator, lb/s
F_{gasoline} = gasoline flow rate from the main fractionator, lb/s
F_{oil} = gas oil feed flow rate, lb/s
F_{product} = total product flow rate from the main fractionator, lb/s
F_{rgc} = flow rate of regenerated catalyst, lb/s
$F_{\text{sucn,comb}}$ = combustion air blower inlet suction flow, ICFM
$F_{\text{sucn,lift}}$ = lift-air blower inlet suction flow ICFM
$F_{\text{surge,lift}}$ = lift-air blower surge flow, ICFM
F_{wg} = flow rate of wet gas to wet gas compressor, lb/s
F_5 = flow of fuel to furnace, SCF/s
i = 1–10, lumps in the ten-lump model: 1-P_h, 2-N_h, 3-C_{Ah}, 4-A_h, 5-P_l, 6-N_l, 7-C_{Al}, 8-A_l, 9-G lump, 10-C lump; 13–18, species in the light gas: 13-butane, 14-butene, 15-isobutane, 16-propylene, 17-N-propane, 18-Gases $\leq C_2$.
k = reaction rate of depletion of oxygen, lb oil (s)/lb catalyst
k_c = frequency factor for the formation of coke, lb coke/lb catalyst^{2,4}
k_{O_2} = frequency factor for the depletion of oxygen in the regenerator, lb coke (s)/ft^3
k_1 = kinetic frequency factor for the formation of gasoline, lb oil (s)/lb catalyst
k_2 = frequency factor for conversion of feed in three-lump model, lb oil(s)/lb catalyst
K = light gas scaling constant, 0.01
L_{sp} = level of catalyst in standpipe, ft
MW = molecular weight (lb/lb mol)
$O_{2,\text{air}}$ = mole fraction of O_2 in air, 0.21
$O_{2,\text{ref}}$ = mole percent oxygen reference, 0.007711 for API = 27; 0.01489 for API = 23
$O_{2,\text{sg}}$ = concentration of oxygen in regenerator stack gas, mol%
p_{feed} = cost of gas oil feed, $/lb
p_i = product value used in the objective function, $/lb
p_{oct} = differential gasoline octane value used in objective function, $/lb/octane number
P_4 = reactor pressure, psia
P_6 = regenerator pressure, psia
Q_{loss} = heat loss from furnace, Btu/s
Q_{total} = total heat generated in furnace, Btu/s
Q_{trans} = heat transferred to feed oil, Btu/s
R = universal gas constant (10.73 ft^3 psia/lb mol/°R)
sa = actual speed of lift air blower, RPM
t_c = catalyst residence time in riser, s
T_{air} = temperature of air entering regenerator, 270°F
T_o = temperature of catalyst and feed entering riser, °F
T_r = temperature at the outlet of the riser, °F
$T_{r,\text{avg}}$ = average temperature in riser used in yield optimization model, °F
$T_{r,\text{ref}}$ = base temperature for reactor riser energy balance, 999°F
T_{reg} = temperature of regenerator bed, °F
$T_{\text{reg,ref}}$ = regenerator reference temperature, 944°F
T_1 = temperature of fresh feed entering furnace, °F
T_2 = temperature of fresh feed entering reactor riser, °F
T_3 = furnace firebox temperature, °F
UA_f = furnace overall heat-transfer coefficient, 25 Btu/s/°F
v_s = superficial velocity in regenerator, ft/s
wt_{ir} = weight fraction of ten lump species, lb/lb feed
$X_{\text{wt.}}$ = weight fraction conversion
X_v = volume fraction conversion
z_{bed} = height of catalyst bed in regenerator, ft
ΔH_{coke} = heat of combustion of coke, Btu/lb coke
ΔH_u = heat of combustion of furnace fuel 1,000 Btu/SCF
ΔP = pressure difference between regenerator and reactor, psig
ρ_B = volume fraction of catalyst in the regenerator
ρ_{feed} = density of gas oil feed to riser (lb/ft^3)
ρ_i = density of light gas component i, lb/ft^3

Literature Cited

Arbel, A., Z. Huang, I. H. Rinard, R. Shinnar, and A. V. Sapre, "Dynamics and Control of Fluidized Catalytic Crackers. 1. Modeling of the Current Generation of FCC's," *Ind. Eng. Chem. Res.*, **34**, 1228 (1995).

Blanding, F. H., "Reaction Rates in Catalytic Cracking of Petroleum," *Ind. Eng. Chem.*, **45**, 1186 (1953).

Corma, A., J. Juan, J. Martos, and J. M. Soriano, "Product Distribution, Kinetics, and Catalyst Decay in the Cracking of a Gas-Oil on a REHY Ultra-Stable Zeolite, and its Comparison with Amorphous and Crystalline Catalysts," 8th Int. Cong. on Catal. (Berlin), II, 293 (1984).

Cutler, C., "Real-Time Optimization and Control of Fluid Catalytic Cracking Units," DMC Corp., Houston, TX (1990).

Desai, P. H., and R. P. Haseltine, "Advanced Catalyst Formulations can be Used to Boost Motor Octane Number of Gasoline," *Oil Gas J.*, **87**, 68 (Oct. 23, 1989).

Ellis, R. C., III, "Supervisory Optimization of a Fluidized Catalytic Cracking Unit," MS Thesis, Texas Tech University, Lubbock (1996).

Ford, W. D., R. C. Reineman, I. A. Vasaloc, and R. J. Fahrieg, "Modeling Catalytic Cracking Regenerators," NPRA Annual Meeting, San Antonio, TX (1976).

Gary, J. H., and G. E. Handwerk, *Petroleum Refining: Technology and Economics*, Marcel Dekker, New York (1983).

Gill, P. E., W. Murray, M. A. Saunders, and M. H. Wright, *User's Guide for NPSOL (version 4). A Fortran Package for Nonlinear Programming*, Systems Optimization Laboratory, Stanford, Palo Alto, CA (1986).

Gross, B. D., D. M. Nace, and S. E. Voltz, "Application of Kinetic Model for Comparison of Catalytic Cracking in a Fixed Bed Microreactor and a Fluidized Dense Bed," *Ind. Eng. Chem. Process Des. Develop.*, **13**, 199 (1974).

Hindmarsh, A. C., "LSODE and LSODI, Two New Initial Value Ordinary Differential Equation Solvers," *ACM SIGNUM Newsletter*, **15**, 11 (1980).

Jacob, S. M., B. Gross, S. E. Voltz, and V. W. Weekman, Jr., "A Lumping and Reaction Scheme for Catalytic Cracking," *AIChE J.*, **22**, 701 (1976).

John, T. M., and B. W. Wojciechowski, "On Identifying the Primary and Secondary Products of Catalytic Cracking of Neutral Distillates," *J. of Catal.*, **37**, 240 (1975).
Khandalekar, P. D., "Control and Optimization of Fluidized Catalytic Cracking Process," MS Thesis, Texas Tech University, Lubbock (1993).
Khandalekar, P. D., and J. B. Riggs, "Nonlinear Process Model Based Control and Optimization of a Model IV FCC Unit," *Comput. Chem. Eng.*, **19**, 1153 (1995).
Krambeck, F. J., "Continuous Mixtures in Fluid Catalytic Cracking and Extensions," Mobil Workshop on Chemical Reaction in Complex Mixtures, Van Nostrand Reinhold, New York (1991).
Lauks, U. E., P. J. Vasbinder, P. J. Valkenburg, and C. van Leeuwen, "On-Line Optimization of an Ethylene Plant," *Comput. Chem. Eng.*, European Symposium on Computer Aided Process Engineering, CACE 16 Suppl. P, S213 (1993).
Lee, E., and F. R. Groves, Jr., "Mathematical Model of the Fluidized Bed-Catalytic Cracking Plant," *Trans. Soc. Comput. Simulat.*, **2**, 219 (1985).
Lee, P. L., and G. R. Sullivan, "Generic Model Control," *Comput. Chem. Eng.*, **12**, 573 (1988).
Leuenberger, E. L., "Optimum FCC Conditions Give Maximum Gasoline and Octane," *Oil Gas J.*, **86**, 45 (Mar. 21, 1988).
Liguras, D. K., and D. T. Allen, "Structural Models for Catalytic Cracking: Reactions of Simulated Oil Mixtures," *Ind. Eng. Chem. Res.*, **28**, 674 (1989).
Liguras, D. K., and D. T. Allen, "Sensitivity of Octane Number to Catalytic Cracking Rates and Feedstock Structure," *AIChE J.*, **36**, 1617 (1990).
Liguras, D. K., M. Neurock, M. T. Klein, S. Stark, A. Nigam, H. C. Foley, and K. R. Bischoff, "Monte Carlo Simulation of Complex Reactive Mixtures: A FCC Case Study," *AIChE Symp. Ser.*, K. C. Chuang, G. W. Young, and R. M. Bensley, eds., **291**, 88 (1992).
McFarlane, R. C., R. C. Reinemann, J. F. Bartere, and C. Georgakis, "Dynamic Simulator for a Model IV Fluid Catalytic Cracking Unit," *Comput. Chem. Eng.*, **17**, 275 (1993).
Maples, R. E., *Petroleum Refinery Process Economics*, Penwell, Tulsa, OK (1993).
Monge, J. J., and C. Georgakis, "Multivariable Control of Catalytic Cracking Processes," *Chem. Eng. Commun.*, **61**, 197 (1987).
Nelson, W. L., "Modern Cracking-Plant Average Yield Data," *Oil Gas J.*, **71**, 86 (1973).
Pierce, V. E., and A. K. Logwinuk, "Which Route to More Octane?," *Hydrocarbon Proc.*, **64**, 75 (1985).
Rhinehart, R. R., and J. B. Riggs, "Two Simple Methods for On-Line Incremental Model Parameterization," *Comput. Chem. Eng.*, **15**, 181 (1991).
Riggs, J. B., *An Introduction to Numerical Method for Chemical Engineers*, 2nd ed., Texas Tech University Press, Lubbock (1994).
Theologos, K. N., I. D. Nikou, A. J. Lygeros, and N. C. Markatos, "Simulation and Design of Fluid Catalytic-Cracking Riser-Type Reactors," *AIChE J.*, **43**(2), 486 (1997).
Van Wijk, R. A., and M. R. Pope, "Advanced Process Control and On-Line Optimization in Shell Refineries," *Comput. Chem. Eng.*, European Symposium on Computer Aided Process Engineering, CACE 16 Suppl. P, S69 (1993).
Voorhies, A., Jr., "Carbon Formation in Catalytic Cracking," *Ind. Eng. Chem.*, **37**, 318 (1945).
Voorhies, A., Jr., C. N. Kimberin, Jr., and W. M. Smith, "Fluid Cracking Catalyst Designed to Maximize Liquid Yields," *Oil Gas J.*, **62**, 108 (1964).
Wacetel, S. J., L. A. Baillie, R. L. Foster, and H. E. Jacobs, "Atlantic Richfield's Lab Unit Apes Fluid Catalytic Cracker," *Oil Gas J.*, **70**, 104 (1972).
Weekman, V. W., Jr., and D. M. Nace, "Kinetics of Catalytic Selectivity in Fixed, Moving, and Fluid Bed Reactors," *AIChE J.*, **16**, 397 (1970).
Winn, F. W., "Physical Properties by Nomogram," *Petroleum Refiner*, **36**(2), 157 (1957).

Manuscript received Feb. 23, 1998, and revision received July 6, 1998.